Steel and Composite Structures, *Vol. 26, No. 6* (*2018*) *745-757*
DOI: https://doi.org/10.12989/scs.2018.26.6.745

Repair of seismically damaged RC bridge bent with ductile steel bracing

Ramiro Bazaez [*1] and Peter Dusicka [2a]

[1] *Departamento de Obras Civiles, Universidad Técnica Federico Santa María, Valparaíso, Chile*
[2] *Department of Civil and Environmental Engineering, Portland State University, Portland, OR, USA*

(*Received August 5, 2017, Revised December 11, 2017, Accepted January 18, 2018*)

Abstract. The inclusion of a ductile steel bracing as means of repairing an earthquake-damaged bridge bent is evaluated and experimentally assessed for the purposes of restoring the damaged bent's strength and stiffness and further improving the energy dissipation capacity. The study is focused on substandard reinforced concrete multi-column bridge bents constructed in the 1950 to mid-1970 in the United States. These types of bents have numerous deficiencies making them susceptible to seismic damage. Large-scale experiments were used on a two-column reinforced concrete bent to impose considerable damage of the bent through increasing amplitude cyclic deformations. The damaged bent was then repaired by installing a ductile fuse steel brace in the form of a buckling-restrained brace in a diagonal configuration between the columns and using post-tensioned rods to strengthen the cap beam. The brace was secured to the bent using steel gusset plate brackets and post-installed adhesive anchors. The repaired bent was then subjected to increasing amplitude cyclic deformations to reassess the bent performance. A subassemblage test of a nominally identical steel brace was also conducted in an effort to quantify and isolate the ductile fuse behavior. The experimental data from these large-scale experiments were analyzed in terms of the hysteretic response, observed damage, internal member loads, as well as the overall stiffness and energy dissipation characteristics. The results of this study demonstrated the effectiveness of utilizing ductile steel bracing for restoring the bent and preventing further damage to the columns and cap beams while also improving the stiffness and energy dissipation characteristics.

Keywords: bridge bent; buckling-restrained brace; repair; reinforced concrete; subassemblage; testing

1. Introduction

Bridges are an important component of a highway network. Interruption and even restriction in traffic caused by excessive damage in a bridge after an earthquake can have severe consequences on the transportation services, the economic activities around the geographic area, and also on the prompt response of emergency vehicles to provide first aid and evacuation services in a timely manner. Moreover, recent earthquakes have demonstrated that damage in structures is not only caused by the initial earthquake strong motion, but also by the subsequent aftershocks (Kam *et al*. 2011, Kawashima and Buckle 2013, Dong and Frangopol 2015, Jeon *et al*. 2016, Abdelnaby 2017). These results in the need to develop repair techniques capable of minimizing the impact on the disruption of traffic, provide effective capacity to sustain aftershocks or subsequent earthquakes, and potentially enhance resiliency of the transportation network.

Post-earthquake reconnaissance of damaged structures often reports visual damage that varies from minor cracks to considerable damage such as complete crushing of concrete, longitudinal rebar buckling and bar fracture. In general, repair of earthquake-damaged reinforced concrete (RC) elements depends on the severity of the damage. In the case of bridge RC components, such as columns and cap beams in which bar fracture had not occurred, repair techniques typically involve epoxy injection into concrete cracks, removal of loose concrete along with patching of spalled zones, and encasing the concrete with FRP wrapping, RC jackets, steel jackets, and prestressing strands provide passive or active confinement (Chai *et al*. 1991, Saadatmanesh *et al*. 1997, Chang *et al*. 2004, Vosooghi and Saiid Saiidi 2013, Fakharifar *et al*. 2016). Once the longitudinal bar has buckled or fractured, repair techniques usually include the replacement of the fractured bars through the use of mechanical splices, reinstallation of transverse reinforcement, and enhancing the concrete confinement through the same methods previously mentioned (Lehman *et al*. 2001, Cheng *et al*. 2003, Shin and Andrawes 2011, He *et al*. 2013).

More recently, buckling restrained braces (BRBs) have been proposed and studied as a structural fuse for seismic retrofitting of bridge bents where they are inserted within the bent to resist primarily the transverse movement of the bridge as conceptualized in Fig. 1 (El-Bahey and Bruneau 2011, Bazaez and Dusicka 2016a, 2017, Wei and Bruneau 2016, Wang *et al*. 2016). The longitudinal movement can often be significantly lower in continuous highway bridges that engage the end abutments. The BRBs themselves are typically composed of a steel core and an encasing system that is isolated from the steel core. The main function of the steel core is to transfer the axial force, while the encasing system prevents buckling of the core under compression,

*Corresponding author, Ph.D.,
E-mail: ramiro.bazaez@usm.cl
[a] Associate Professor, Ph.D., E-mail: dusicka@pdx.edu

ISSN: 1229-9367 (Print), 1598-6233 (Online)

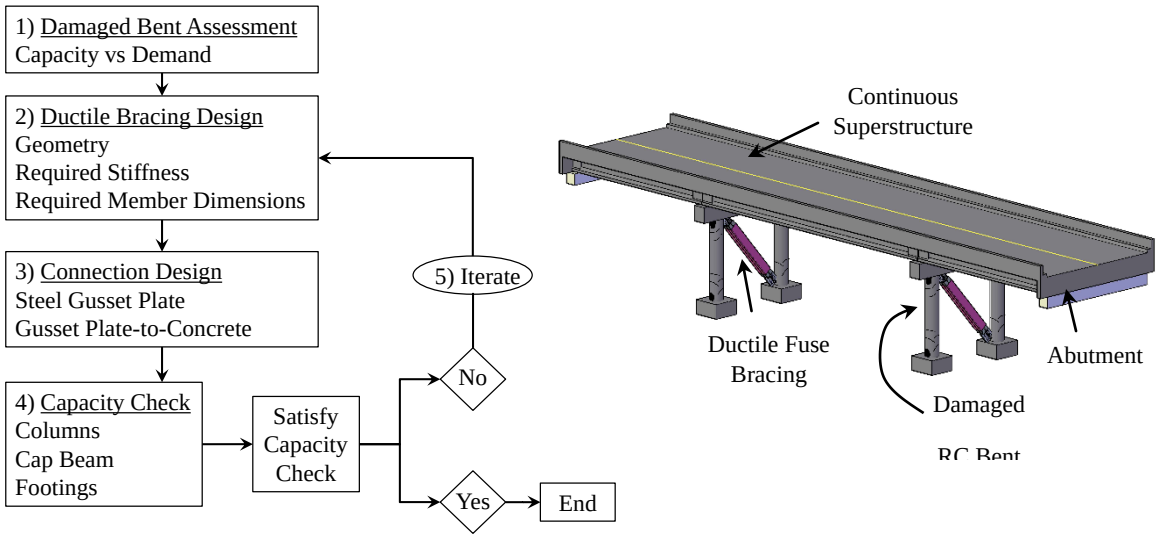

Fig. 1 Design steps for repair using ductile steel bracing

resulting in stable hysteretic behavior in both tension and compression. Despite the increasing use of BRBs in buildings and the recent interest for applying them for retrofitting RC bridges, their use as a repair technique has not been studied. The objective of this study is to propose a framework for designing structural steel ductile fuse bracing for earthquake-damaged RC multi-column bridge bents and to experimentally investigate the effectiveness of this post-earthquake repair.

2. Design of ductile fuse bracing as repair technique

The aim for implementing the structural ductile fuse in damaged RC bents is threefold: (1) to restore the strength and stiffness to the damaged structure; (2) to increase the energy dissipation capacity of the structure going forward, while limiting the damage in the remaining components to preserve the bridge serviceability; and (3) to provide the system a mechanism capable of sustaining subsequent earthquakes or aftershocks. As in any design, in order to effectively repair damaged RC multi-columns bridge bents, iteration is required until all the limit states of each component are verified and a suitable design is found. For this purpose a general repaired procedure with 5 steps is suggested as shown in Fig. 1. The proposed repair outlined in this paper is primarily intended for bents where significant buckling and rupture of the main reinforcing steel have not yet occurred. However, if the longitudinal reinforcing steel did buckle or fracture, repair techniques involving replacement of the fractured bars and reinstallation of transverse reinforcement could be utilized in conjunction with the incorporation of the ductile steel bracing.

Step 1: Assess the damaged structure in an effort to determine the level of damage and the residual strength and stiffness of the structure. FEMA306 (1998) and FEMA307 (1998) suggest the use of a modified plastic hinge model to

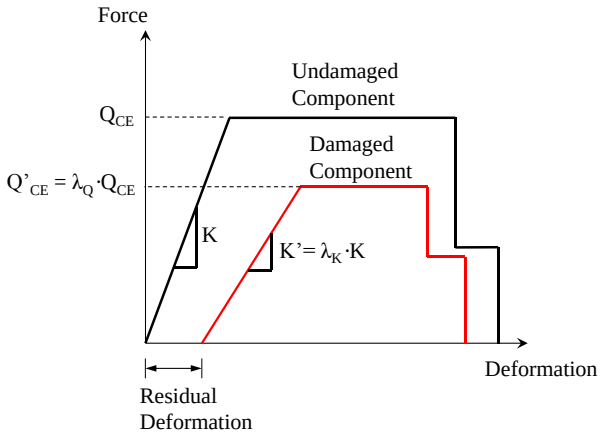

Fig. 2 Modeling of damaged components

account for the reduced strength, reduced stiffness and the residual deformation of the damaged component, similar to that shown in Fig. 2 where, K and Q_{CE} are the stiffness and strength of the undamaged component, respectively. K' and Q'_{CE} are the stiffness and strength of the damaged component, respectively. λ_K is a stiffness modification factor that accounts for change in effective initial stiffness resulting from damage, and λ_Q is a modification factor that accounts for change in expected strength resulting from damage.

Based on FEMA306 and 307, the modification factors can be stablished from experimental results of critical components or using the recommendations summarized in Table 1. The modification factors for damaged substandard RC columns were investigated and experimental data based formulations were introduced based on 23 experiments conducted on substandard columns with deformed bars and 13 substandard columns with smooth bars (Di Ludovico *et al*. 2013). Based on this data, Eqs. (1)-(2) were proposed for the stiffness and strength factors, respectively, to be used on the theoretical assessment of the residual capacity using pushover analyses.

Table 1 Modification factors for damaged RC components

Mode of failure:	Ductile flexural			
Damage severity	Insignificant (minor cracks)	Slight (crack width < ¼ in)	Moderate (spalling)	Heavy
λ_K	0.8	0.6	0.5	Not used
λ_Q	1.0	1.0	0.8	Not used

$$\lambda_k = 1 - \left[1.01 - 0.96 \cdot \left(\frac{\theta}{\theta_y}\right)^{-1.1}\right] \quad \text{for} \quad 1.0 < \theta/\theta_y \leq \theta_u/\theta_y \tag{1}$$

$$\lambda_Q = 1 - 0.05 \cdot \left(\frac{\theta}{\theta_y} - 3.9\right) \quad \text{for} \quad 3.9 < \theta/\theta_y \leq \theta_u/\theta_y \tag{2}$$

Where θ is the peak rotation (or drift) of the component, θ_y is the yield rotation (or drift) and θ_u is the ultimate rotation (or drift). A preliminary assessment of the residual strength and stiffness of the damaged structure is recommended to be computed using the information presented in Table 1. However, a more detailed design can be performed using Eqs. (1)-(2).

Step 2: Determine the location, configuration, stiffness and dimensions of the ductile steel bracing. With that aim BRBs need to be designed following a structural fuse concept, which aims to maintain the primary gravity resisting system within primarily the elastic range. However, the post-earthquake state of the RC bents means that critical components have already yielded and suffered damage, resulting in degraded stiffness. Hence satisfying the condition of limiting the maximum displacement demand of the repaired bent below the yield displacement of the undamaged as-built RC bent as stated in an ideal structural fuse design is not feasible. Thus, larger inelastic excursions can be allowed within a reasonable range in an effort to still provide for a ductile response without considerably increasing the damage of the structure as shown in Fig. 3 and expressed in Eq. (3). A displacement of 2 times the yield displacement of the undamaged as-built bent, which means displacement ductility of 2, has been suggested by Priestley *et al*. (1996) and reported in NCHRP Synthesis 440 (2013) in order to achieve an operational (serviceability) performance. This performance level is characterized by limiting the crushing of cover concrete and residual crack width to 1 mm. In this study, a factor of 2.5 applied to the yield displacement of the undamaged bent (displacement ductility of 2.5) is suggested in order to limit further damage on the already damaged structure and still provide for a system ductile response. The design of the brace is determined through iteration until the stiffness of the BRB (K_i^{BRB}) satisfies Eq. (5).

$$\delta^R = R_d S_a g \frac{m}{K_i^{BRB} + \lambda_k k_{eff}^B} \leq 2.5\delta_y^B \tag{3}$$

$$R_d = \begin{cases} (1 - 1/\mu_D) \cdot 1.25T_s/T_e + 1/\mu_D & \text{for } 1.25T_s/T_e > 1.0 \\ 1.0 & \text{for } 1.25T_s/T_e \leq 1.0 \end{cases} \tag{4}$$

$$K_i^{BRB} \geq \frac{R_d S_a m g}{2.5 \cdot \delta_y^B} - \lambda_K k_{eff}^B \tag{5}$$

Where, δ^R is the displacement demand of the repaired system, $\delta_y{}^B$ is the yield displacement of the undamaged bent, T_e is the fundamental period of the system; S_a is the spectral acceleration given by the respective response spectrum; g is the standard gravity constant; m is the inertial mass of the system, $k^B{}_{eff}$ is the effective stiffness of the undamaged bent, T_s is the period at the end of constant design spectral acceleration plateau and μ_D is the maximum local member displacement ductility demand. Once the required BRB stiffness is determined, the yield displacement of the brace ($\delta_y{}^{BRB}$) can be obtained setting a target BRB ductility at the displacement demand of the repaired system. The yield displacement of the brace is found dividing the displacement demand by the target BRB ductility. Then, the required horizontal strength of the brace ($V_y{}^{BRB}$) is obtained by multiplying the brace yield displacement by the BRB stiffness ($V_y{}^{BRB} = K_i{}^{BRB} \cdot \delta_y{}^{BRB}$). The implementation of this repair technique can be applied

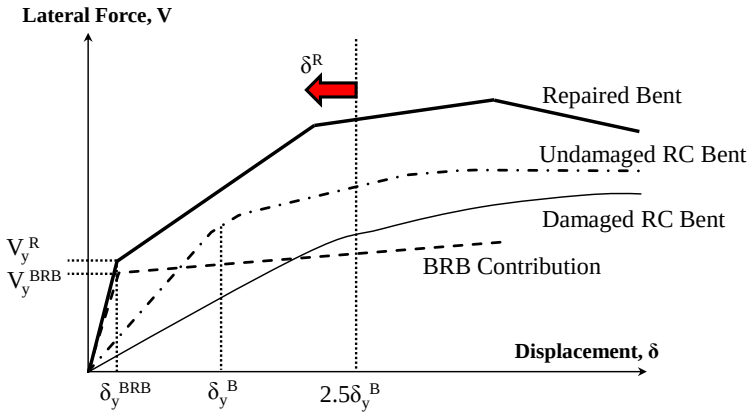

Fig. 3 BRBs as seismic repair for damaged RC bents

to any earthquake-damaged RC bent. Depending on the type of bridge and the abutment condition, additional repair techniques may be necessary in the longitudinal direction.

Step 3: Connections between the BRB and RC elements need to be designed based on capacity design to sustain the load transferred from the fuse element. The design involves designing the connection between brace to gusset plate and gusset plate to concrete components.

Step 4: Column, cap beam and footing capacity need to be re-checked to ensure that the structure is capable of sustaining the demands generated by including the BRB and an acceptable mechanism of collapse is achieved.

Step 5: If the capacity of any component of the bent is not satisfied, repeat steps 2 to 4 as needed to converge on a design.

3. Experimental program

3.1 Specimen description

The representative RC bent utilized in this study corresponds to a commonly found multi-column bridge bent constructed in the 1950 to 1970 in the Pacific Northwest of the United States. As many of the bridge structures built at that time, the bridge bent was designed and built with minimum seismic considerations. This resulted in inadequate transverse reinforcement and confinement, no seismic detailing, and presence of lap-splices within plastic hinge zones. In order to represent the typical RC bridge bent, a large-scale bent specimen, hereinafter referred to as "As-built" was designed using geometric similarity with a scale factor of 0.5. The large-scale bent specimen consisted of two 457 mm diameter circular columns and a rectangular 457 mm × 533 mm cap beam. The longitudinal reinforcement in the columns consisted of 10 ϕ16 mm bars equally spaced. The transverse hoop reinforcement was deformed wire ϕ6.4 mm spaced at 152 mm center to center. Lap splices were located at the base of the test specimens through the incorporation of 10 ϕ16 mm dowels. The lap splice length replicated the detailing in the representative bridge, which is roughly 40 times the diameter of the longitudinal steel reinforcement ($40d_b$). The reinforcing steel used to construct the test specimens consisted of Grade 40, f_y = 276 MPa, f_u = 414 MPa, deformed bar conforming ASTM A615.

Table 2 Measured material properties

Element	Parameter	Measured value
Rebar ϕ16 mm	$f_{y\text{-}me}$ (MPa)	345
	$f_{u\text{-}me}$ (MPa)	523
	Elongation, %	17.5
Wire ϕ6.4 mm	$f_{y\text{-}me}$ (MPa)	-
	$f_{u\text{-}me}$ (MPa)	538
	Elongation, %	6
Column (As-built)	$f'_{c\text{-}me}$ (MPa)	33.9
Colum (Repaired)		33.8
Beam (As-built)		32.9
Beam (Repaired)		32.9
BRB	f_y (MPa)	299

Normal weight concrete was used to construct the test specimens with a target 28-day strength (f'_c) of 22.8 MPa. The concrete cover was 25.4 mm for columns and 19 mm for the cap beam. Standard compression testing of 152 mm by 305 mm concrete cylinders was performed at 7-day, 28 days and at the day of test completion. The average concrete compressive strength, the yield ($f_{y\text{-}me}$) and tensile ($f_{u\text{-}me}$) stress, and the elongation of the reinforcing steel obtained from tensile tests are shown in Table 2. It is worth noting that the measured values of $f'_{c\text{-}me}$ are close to the assessment strengths, $f'_{ca} = 1.5f'_c = 34.1$ MPa, suggested by Priestley for existing bridges. (Priestley *et al*. 1996)

The BRB design of the specimen was performed following the above described structural fuse concept. To account for the reduced stiffness and strength of a damaged bent, a stiffness factor (λ_k) equal to 0.5 and a strength factor (λ_Q) equal to 0.8 were applied to the stiffness and strength of the undamaged bent. These factors were assumed in an effort to represent the stiffness when the concrete has already spalled. For the brace, a yield stress of 299 MPa given by the BRB manufacturer, a brace angle (θ) of 48.7 degrees and a BRB length of 3318 mm were considered for this application. The repaired bent was designed for a response spectrum with maximum spectral acceleration (S_a) equal to 0.85 g and with a period at the end of constant design spectral acceleration plateau (T_s) equal to 0.53 sec. The area of the BRB steel core within the reduced section and the length of the reduced section (L_c) for the BRB were selected as 774 mm^2 and 1750 mm, respectively.

3.2 Test setup layout

The test setup used in this study was similar to the one described in Bazaez and Dusicka (2016a), where the cyclic lateral loading was applied through a horizontal hydraulic actuator attached to a steel connector beam at the bent cap level. Illustrations of the test setup for the as-built and repaired bents are shown in Fig. 4. Compressive loads equal to 10% of the nominal column axial capacity ($0.10f'_cA_g$ = 373.5 kN) were applied to simulate the superstructure dead load on the columns.

Unconstraint steel gusset plates composed of steel plates ASTM A572 Gr. 50 were used in the connection between the BRBs and the horizontal reinforced concrete elements. The steel brackets were intentionally not connected to the columns by including a gap of 25 mm between the steel brackets and the RC columns (Bazaez and Dusicka 2016a, 2017). A six degree of freedom (6DOF) load cell was integrated at mid-span of the cap beam in order to directly measure the internal forces that were transmitted from one side of the bent to the other, and thereby allow for indirect calculation of the internal loads within the bent, including the axial force in the BRB. The bent was fully instrumented via linear variable displacement transducers (LVDTs), string pots, strain gauges, and load cells.

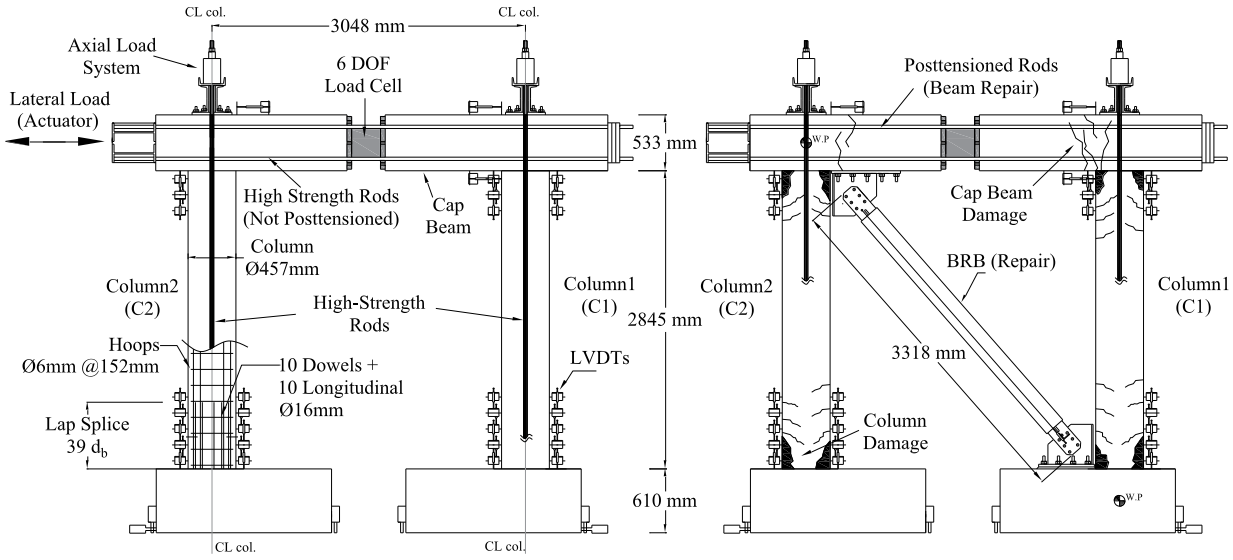

(a) As-built bent (b) Repaired bent

Fig. 4 Bridge bent test specimens

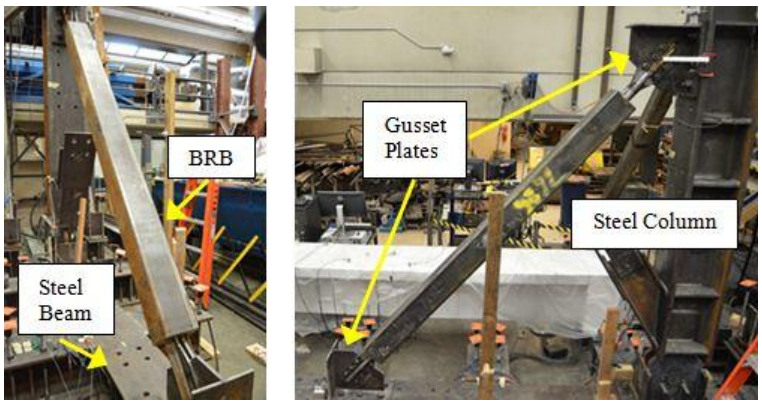

Fig. 5 Subassemblage test setup

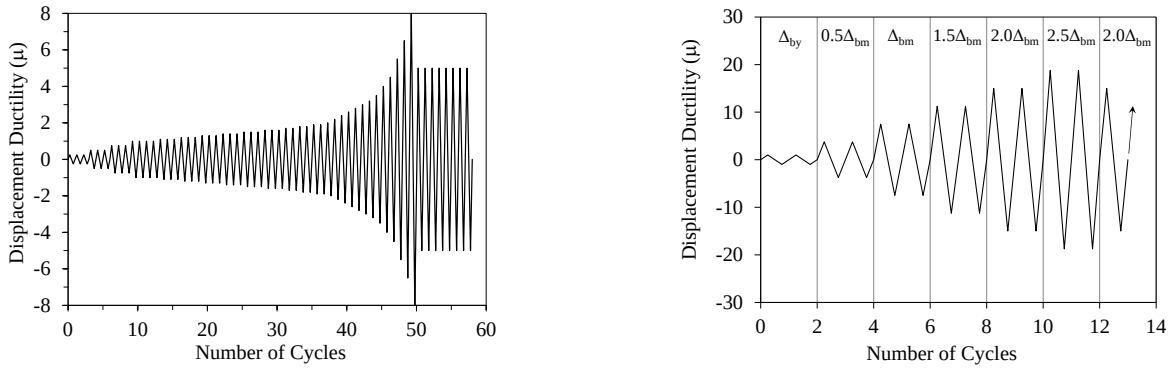

(a) As-built and Repaired bents (b) Subassemblage test

Fig. 6 Cyclic loading histories

In order to evaluate a nominally identical BRB to that used in the repaired system, a subassemblage test was performed on the BRB with similar gusset plate brackets boundary conditions as those implemented in the RC bent repair. The subassemblage test setup comprised of a steel beam connected to a strong floor, a steel column pinned at its base, a hydraulic actuator, two gusset plates and a BRB specimen as shown in Fig. 5. The specimen was instrumented with displacement transducers (LVDTs) to measure the BRB axial deformation (Δ). LVDTs were also

utilized to monitor potential slippage in the BRB-gusset plate connection, out-of-plane displacement of the gussets, uplift of gussets, and slippage between gusset plate and steel beam/column. String pots were utilized to measure the total lateral displacement of the system, and to monitor any significant out-of-plane displacement of the BRB in an effort to assess potential global buckling.

3.3 Loading sequence

The test sequence comprised of testing an initially undamaged RC As-built Bent until moderate to severe damage was achieved. The bent was then repaired by adding a BRB in a diagonal configuration as the ductile fuse brace and posttensioning the horizontal high-strength rods in the cap beam. Then, the second test was carried out, hereinafter referred to as the Repaired Bent test. Both tests were conducted using cyclic loading that was developed to reflect subduction zone earthquake displacements, which is one of the main earthquake hazards in the Pacific Northwest of the United States (Bazaez and Dusicka 2016b). The specific cycles described by this loading protocol are dependent on the fundamental period. The cycles applied to the bent specimen were selected based on an assumed fundamental period of 0.5 sec, which was found to be representative of highway bridges with unbraced multi-column bents. The repaired bridge was assumed to exhibit a restored stiffness and for comparisons purposes, the same loading protocol was again utilized for the repaired case. The resulting horizontal displacements were applied via progressively increasing cycles as shown in Fig. 6(a). The system displacement ductility was defined as $\mu = \delta/\delta_y$, where δ is the top lateral displacement at a specific cycle and δ_y is the yield displacement of the system. The nominal yield displacement was initially calculated from material properties for all the specimens and then corrected on each test.

The loading protocol applied to the subassemblage test was based on the BRB qualification loading protocol of AISC (2016). This loading protocol shown in Fig. 6(b) was adopted despite being intended for building frames as there are no other established protocols and the main purpose was to establish brace characteristics including measured yield and over-strength. The loading history was controlled by the axial deformation at first significant yield (Δ_{by}) and the axial deformation corresponding to the design drift (Δ_{bm}). The first significant yield (Δ_{by}) was calculated using the nominal properties of the brace. The design drift (Δ_{bm}) was computed using $7.5\Delta_{by}$. The values of Δ_{by} and Δ_{bm} were 2.5 mm and 16.6 mm, respectively. The AISC protocol requires that after the initial two cycles at $2\Delta_{bm}$, additional complete cycles of loading at a deformation corresponding to Δ_{bm} be performed as required for the brace test specimen to achieve a cumulative inelastic axial deformation (CID) of at least 200 times the yield deformation. Even though these additional cycles are not required for the subassemblage test specimen, in this study, additional two cycles at $2.5\Delta_{bm}$ and then multiple cycles at $2.0\Delta_{bm}$ were performed in an effort to achieve a cumulative inelastic axial deformation of at least 350 times the yield deformation. Failure of the brace was defined as the point when a strength degraded by 20% of the peak load.

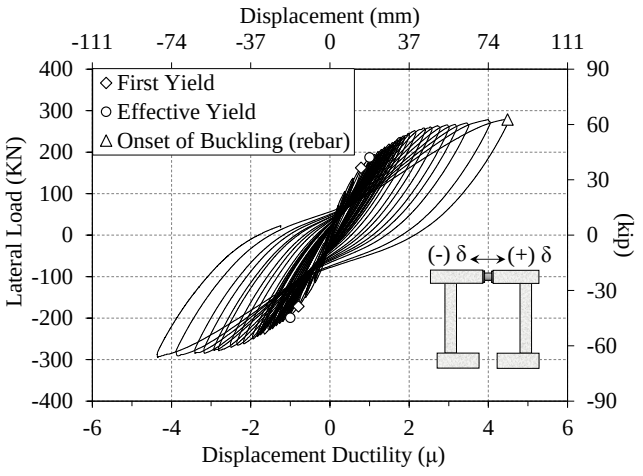

Fig. 7 Hysteretic response of As-built Bent

4. Experimental results and discussion

4.1 As-built bent response

In order to avoid reaching significant rebar buckling and rupture, the As-built Bent was tested up to a displacement ductility of 4.5. This ductility value was selected based on observed damage and experimental results obtained from the RC bent performance reported in Bazaez and Dusicka (2016a), which suggested that rebar buckling for a similar RC bent would occur at a displacement ductility of 4.8. This level of damage was selected because of the anticipated significant inelasticity, but prior to rebar buckling or rupture. The recorded lateral load-deformation behavior for the As-built Bent is shown in Fig. 7. The peak lateral load was 294 kN and occurred at a lateral displacement of approximately 82 mm. First yield of the longitudinal reinforcement occurred at a displacement of 14 mm based on strain and curvature measurements. The effective yield displacement, which was assumed at the occurrence of change in slope of the load–deformation curve, was computed as 19 mm. The initial damage consisted of horizontal cracks that propagated throughout the height of the expected plastic hinge zones of columns. Also, early formation of vertical cracks were observed in the cap beam at the face of column C1. Vertical cracks in the cap beam increased in width up to 0.6 mm as shown in Fig. 8(a). This observation denoted that a plastic hinge formed in the cap beam, which is prohibited by current specifications but could occur in existing bridges that were not seismically designed. Significant spalling of concrete at expected plastic hinge locations was observed during the last cycles at displacement ductility of 4.5 as shown in Fig. 8(b). Also, vertical cracks were observed at the column base, which can be attributed to the lap splice at that location. Onset of dowel buckling was observed at the base of column C2 during the last cycle at a displacement ductility of 4.5 as depicted in Fig. 8(c). Neither failure of the bars, nor strength degradation had been observed in the specimen at

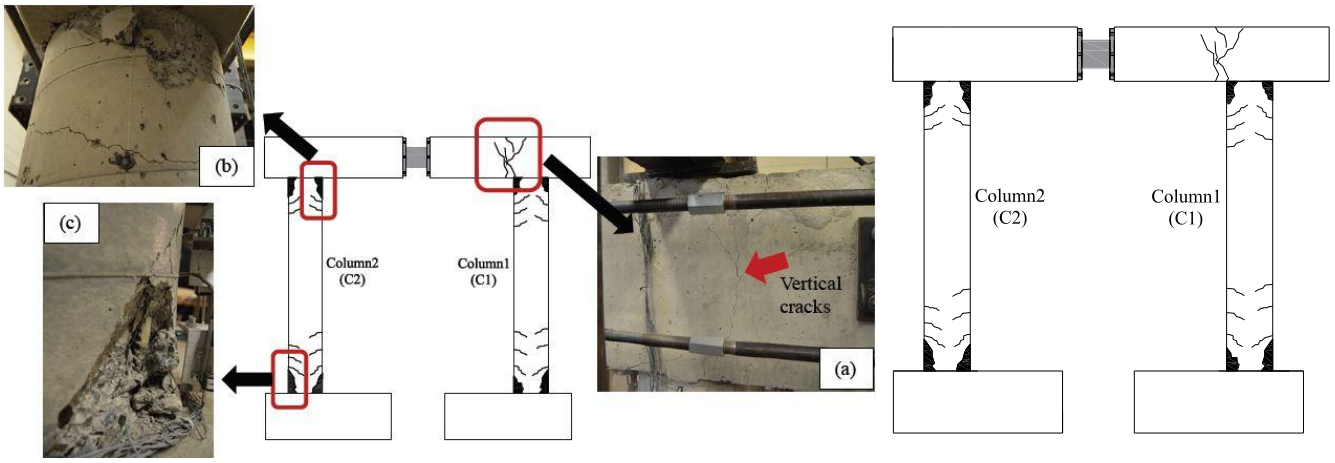

Fig. 8 Imposed Damage in As-built Bent: (a) cap beam cracks; (b) significant spalling in columns, (c) onset of rebar buckling

the end of the test.

4.2 Repaired bent response

The ductile steel brace utilized for repairing of the damaged bent was designed following the structural fuse concept, which resulted in limiting the displacement of the bent and preventing significant damage in the cap beam and the columns. Given the observed damage of the As-built bent, repairing of the cap beam was also needed. The cap beam was repaired by increasing the compressive axial stresses, which was accomplished using posttensioned rods as shown in Fig. 4(b). The increased compressive stresses thereby increased the capacity of both the cap-beam and the beam-column joint. The posttensioning force was applied using 4 horizontal high-strength rods spanning between plates at the ends of the cap beam. The compressive force of 311 kN applied to the cap beam was calculated with the aim of restricting further damage in that component. While repair of the bent would also involve concrete repair around the spalled areas, no additional structural or even cosmetic repairs were conducted so as to be able to observe potential subsequent damage of the bent. This decision was a conservative approach taken for the experiments. Patching of spalled concrete can be implemented in field installations, but repair to full capacity of the existing columns is unnecessary due to displacement compatibility as the bent no longer relies on the moment capacity and energy dissipation of the RC columns. Potential issues can arise at the installation of the steel brackets via post-installed anchors if the connection areas in the bent beam or foundation are damaged. In those case, these areas may also need to be repaired prior to installing the brackets. Repair methods may include epoxy injection into concrete cracks, removal of loose concrete along with patching of spalled zones, and encasing the damaged zones with RC, FRP or externally applied steel. It is also worth mentioning that in the laboratory we did not have permanent deformations prior to the installation of the brace. However, if residual drift is measured in the field, the bridge can be plumbed prior to the ductile steel brace install.

The repaired bent was subjected to the loading protocol shown in Fig. 6(a). Initial calculations indicated that the

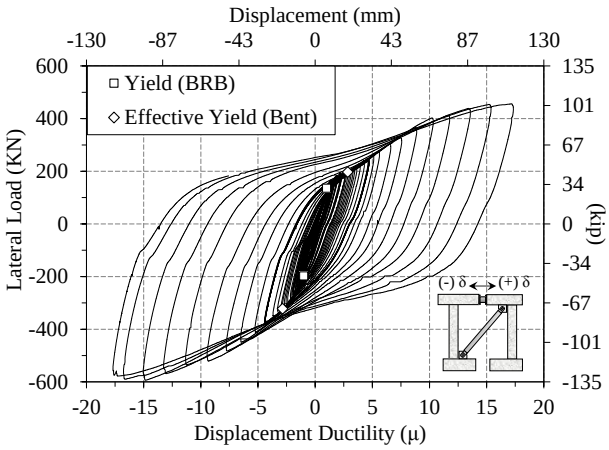

Fig. 9 Hysteretic response of Repaired Bent

maximum displacement demand of the repaired bent for the design target spectra was 30 mm. After completing the test protocol no appreciable damage in the RC components was observed and no degradation of the hysteretic behavior of the bent was recorded. Thus, additional cycles of increasing amplitude were performed after the loading history was completed. The test was stopped after 5 more cycles of increased displacement amplitude mainly because the large amplitude displacements in conjunction with the onset of out-of-plane displacements of the bent caused by the large deformations started to jeopardize the safety of the equipment in the laboratory.

The lateral load vs. deformation hysteresis curve for the repaired bent shown in Fig. 9 indicates highly ductile behavior and high energy dissipation up to a displacement ductility of 17.7, which is equivalent to a displacement of 115 mm. In this case, the displacement ductility was calculated using the yield displacement of the BRB. The nominal lateral displacement at yield for the BRB was calculated as 4.1 mm and the experimental one was 6.6 mm, which is a 61% increase with respect to the nominal value. This difference was caused by the flexibility added by the non-yielding parts of the brace and the gussets. The effective yield of the As-built RC bent is also depicted in Fig. 9 as a point of comparison. As the progressively

(a) Overall damage (b) Buckling of steel (c) Damage in cap beam

Fig. 10 Damage in repaired bent

increasing displacements were applied, the lateral load increased up to 596 kN for the brace compression direction and 458 kN for the brace tension direction. This difference in strength capacity was expected since Fig. 9 shows that the response was dominated by the stable hysteretic behavior of the BRB, which characteristically exhibits more strength capacity in compression due to the additional friction forces exerted in the interface between the steel core and the confining concrete.

Regarding damage progression, at the beginning of the test the columns and cap beam had the same damage shown at the end of the As-built Bent test since no effort was intentionally made to repair that damage. No further damage was registered in the RC components until a displacement ductility of 8, which is equivalent to 53 mm. After that point, crushing of the concrete at the base and top of the columns was recorded, exposing the column reinforcement. Once the concrete cover was lost, the longitudinal bars and dowels in those regions began to buckle as shown in Figs. 10(a) and (b). Despite of the columns sustaining significant damage at the large ductility deformations, the system showed only minor strength deterioration that was particularly noticed in the last cycle when the BRB was in compression. This result presumably indicates that the columns continued to fully resist the imposed gravity loads. Moreover, at the end of the test no further damage was observed in the cap beam as shown in Fig. 10(c), which demonstrates that posttensioning the cap beam was an effective method to restrict the damage in that component. Inspection of the gusset plates, which was conducted following the removal of the BRB, did not reveal any damage.

4.3 Ductile fuse steel brace component response

The elongation of the BRB was measured via four LVDTs. The axial force in the BRB within the bent was indirectly obtained using the measurements from the 6DOF load cell located at mid-span of the beam, the load cells located on top of the rams, and the corresponding free body diagrams considering the post-tensioning force. In order to resolve the brace axial force, shear and moment in the BRB were assumed to be negligible. The resulting BRB response envelope is illustrated in Fig. 11. The numerical bi-linear

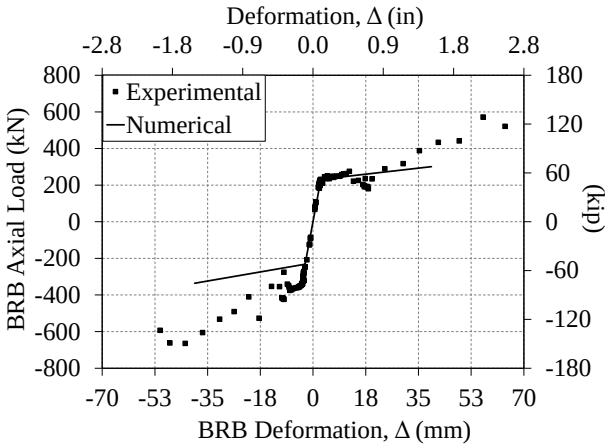

Fig. 11 Brace axial response within the repaired bent

response was computed using nominal material properties and preliminary over-strength factors of 1.3 and 1.45 in tension and compression, respectively, as given by the BRB manufacturer. The BRB deformation in the numerical curve was only extended to $15\Delta_{by}$ since the adjustment factors were computed to that level of deformation. Numerical and measured yield elongation (Δ_{by}) were calculated as 2.5 mm and 4.3 mm, respectively. Comparison of the inferred envelope and the numerically obtained response in Fig. 11 shows that the numerical approximation fits well with the experimental curves in the elastic range. However, in the inelastic range the preliminary over-strength factors underestimated the BRB strength. The estimated maximum axial strain of the steel core at the end of the test was computed by dividing the maximum elongation by the reduced section length, and was approximately 4%. The contribution of the BRB at the peak load of the repaired system was 73%, which showed that more than half of the system maximum lateral load was resisted by the BRB.

4.1.1 Subassemblage test

The brace used in the subassemblage test had a steel core area of 774 mm^2 and a reduced section length of 1750 mm, resulting in the brace shown in Fig. 5. The hysteretic response of this brace shown in Fig. 12 underscores the ductile and stable hysteretic behavior of this BRB, but also

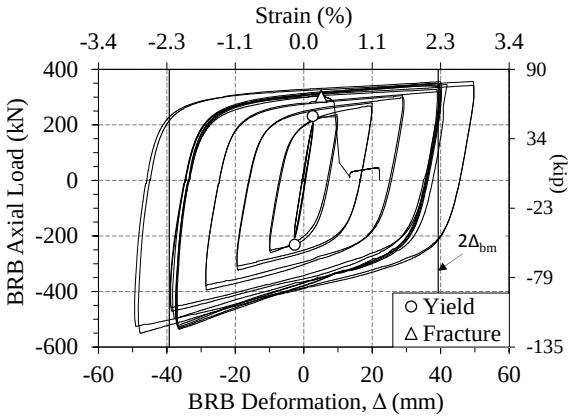

(a) Hysteretic response of BRB

(b) Core elongation of the BRB

Fig. 12 Subassemblage test results

the highly asymmetric characteristics between tension and compression strengths. Peak loads of 356 kN and 552 kN in tension and compression respectively were recorded. In terms of axial deformation, the brace exceeded the minimum deformation required by the AISC seismic provisions (AISC 341-16 2016). The nominal yield deformation of the brace was computed as 2.5 mm and the maximum deformation of the brace was 49.8 mm, which is equivalent to a brace ductility of 19.6. After two cycles at maximum deformation, cycles at an amplitude of $2\Delta_{bm}$ were performed until failure of the specimen was reached. Failure of the specimen was observed after 5 cycles at that amplitude.

No visual damage was observed in the BRB during the test. However, the significant degradation in axial strength at failure as shown in Fig. 12(a) and a permanent residual deformation of the brace measured at the end of the test (Fig. 12(b)) indicates that an internal fracture of the steel core had occurred. Visual inspections after removing the BRB from the test setup showed that the gusset plates did not exhibit any damage despite the larger than anticipated compression achieved by the brace. This result was corroborated with strain gauge measurements that indicated that the gussets remained elastic with a maximum strain of 0.0013, which is lower than the strain at yield (0.0017) for ASTM A572 Gr50 plates.

Over-strength factors

The tension (or strain hardening) over-strength factor, ω, was computed using Eq. (6) and the compression adjustment factor, β, was computed using Eq. (7).

$$\omega = \frac{T_{\max}}{P_y} = \frac{T_{\max}}{f_y \cdot A_{sc}} \tag{6}$$

$$\beta = \frac{P_{\max}}{T_{\max}} \tag{7}$$

In these equations, P_y is the nominal axial force at yield, f_y is the nominal yield stress, A_{sc} is the area of the steel core, $T_{\max}$ is the maximum tension load at each cycle, and $P_{\max}$ is the maximum compressive load. Both strength adjustment factors are shown in Fig. 13 at different displacement ductilities. The figures show that as the displacement ductility increases both factors increase linearly. The maximum factors were computed as 1.54 and 1.57 for the tension over-strength and the compression adjustment factors, respectively. The compression adjustment factor (β)

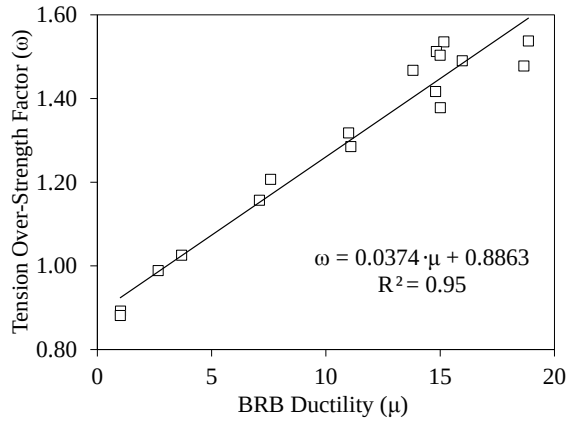

(a) Tension over-strength

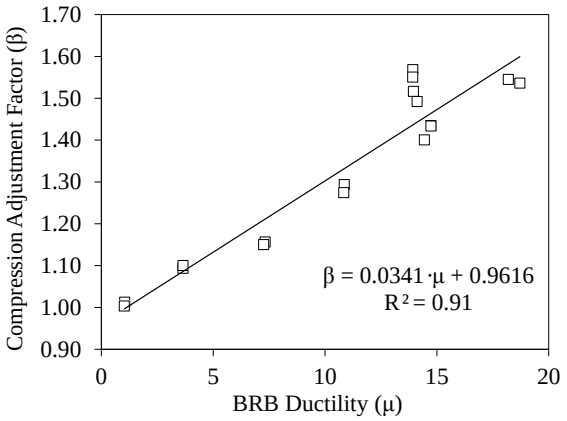

(b) Compression adjustment

Fig. 13 Brace over-strength factors

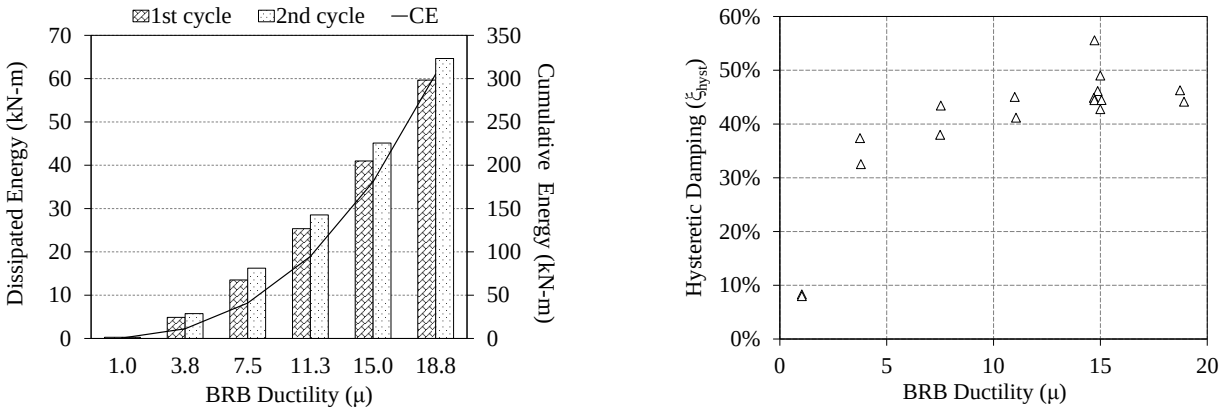

(a) Dissipated energy (b) Hysteretic damping

Fig. 14 Brace Energy dissipation

was found to be significantly larger than the limit of 1.3 that the AISC (2016) guidelines require. Nonetheless, the subassemblage test results corroborated the asymmetric strengths in tension and compression observed during the Repaired Bent test and underscore the importance of controlling the over-strength factors in the design of BRBs.

Cumulative inelastic deformation and energy dissipation

Cumulative inelastic deformation was calculated from the subassemblage tests following the Seismic Provisions of AISC 341-16 (2016). A cumulative inelastic axial deformation of 690 times the yield deformation was calculated for the BRB. This result show that the cumulative inelastic deformation for this BRB was greater than three times of the minimum required for qualification of BRBs, which stipulates a cumulative inelastic deformation of at least $200\Delta_{by}$. This value of cumulative inelastic deformation is important to quantify since a large value indicates that the brace can withstand numerous plastic cyclic deformations.

The energy dissipation attained by the specimen was calculated using the total area enclosed by the hysteretic curves and is depicted in Fig. 14(a). The results show that the cumulative energy dissipated by the brace was more than 300 kN-m and that more energy was consistently dissipated during the second cycle at the same displacement ductility level. The latter result is caused by the characteristic strain hardening that BRBs exhibit. Another important parameter that demonstrates the energy dissipation capacity that a structural component can achieve is the hysteretic damping. The hysteretic damping, shown in Fig. 14(b), was calculated as the ratio of energy dissipated in a full cycle to 4π times the strain energy measured at the average peak force of each cycle. The brace reached a maximum of 55% hysteretic damping before failing. The results also show that large values of damping (> 30%) can be achieved at relatively low BRB ductilities and that at typical brace ductility demands (μ = 6 to 15) the damping is over 40%. In summary, these results demonstrate the desirable energy dissipation capacity that BRBs can attain.

4.4 Bent columns axial load

The internal axial load in column 1 (C1) and column 2 (C2) were calculated by adding the axial load applied on top of each column, the shear measurement of the 6DOF load cell located at the mid-span of the cap beam, and decomposing the axial load contribution from the BRB. The internal axial loads in C1 and C2 for the specimens are shown in Fig. 15. The results showed the influence of the

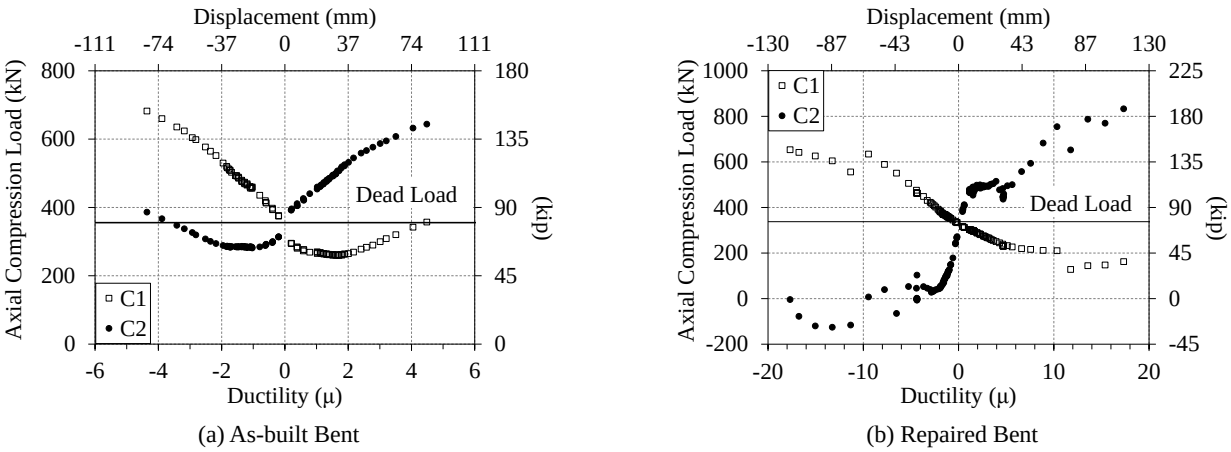

(a) As-built Bent (b) Repaired Bent

Fig. 15 Internal column axial load

BRB on C1 is negligible as compared to the As-built condition. On the contrary, the axial load in C2 is directly affected by the inclusion of the BRB since the axial load in the BRB is decomposed into an additional axial load in that column. The effect is such that at some point C2 is under tension loads as shown in Fig. 15(b). The fact that tension loads were reached in column 2 are a consequence of large BRB compression over-strength factors. The results are also a direct consequence of the brace-to-bent connection, which connected the brace to the footing on one side and to the cap beam on the other. Any significant variation in the internal axial load of columns needs to be accounted for in the repair design and will affect the subsequent assessment of other components.

4.5 Backbone curve comparison

Backbone curves were generated to visualize and understand the difference in terms of initial stiffness, overall load and displacement capacity that the specimens exhibited. Fig. 16 compares the backbone curves from the two experiments in terms of ductility of the As-built bent condition, i.e., ductility one corresponds to the effective yield of the As-built Bent, δ_{ye}, as shown by the vertical dashed lines. For the repaired bent, results showed that the strength increased by 63% in the positive direction and 102% in the negative direction with respect to the maximum strength achieved by the As-built condition. The tangent stiffness at yield also increased by 158% in the repaired condition. Thus, the repaired bent exhibited larger strength and stiffness as compared to the As-built bent, demonstrating that repairing damaged RC bents with BRBs is a feasible option to restore the stiffness and strength of the system.

4.6 Assessment of stiffness modification factor

The stiffness modification factor (λ_k), represented as the secant stiffness (k_{sec}) divided by the stiffness at yield (k_y), was calculated to assess the stiffness degradation of the bent at different displacement ductilities: The secant stiffness was calculated at peak displacement of each cycle. The yield displacement used in the calculations for the stiffness at yield corresponds to the effective yield displacement calculated for the As-built Bent, and the yield displacement of the BRB for the repaired bent as those were the first sign of inelasticity in each case. Fig. 17 shows that the Repaired bent had lower stiffness degradation rate than the As-built Bent, in particular in the positive direction. This lower stiffness degradation of the repaired bent was caused by the stable and highly ductile hysteretic response provided by the BRB within the overall response.

Since stiffness modification factors are used in the design of the repair technique, the experimental stiffness modification factors were compared to the values obtained of using Eq. (8) (Di Ludovico *et al*. 2013) and to the values suggested in FEMA307 (1998) for the assessment of damaged structures.

$$\lambda_k = 1 - \left[1.07 - 1.15 \cdot \left(\frac{\theta}{\theta_y}\right)^{-0.92}\right] \quad \text{for} \quad 1.1 < \theta/\theta_y \leq \theta_u/\theta_y \tag{8}$$

The results summarized in Fig. 17 show that Eq. (8) gives lower stiffness modification factors than the experimental data for any achieved ductility level. This result indicates that applying Eq. (1) or (8) in the design process of the repair technique (i.e., in step 1) may be conservative since larger displacement demands for the repaired bent are expected. On the contrary, the values suggested in FEMA307 (1998) (Table 1) for ductile flexural behavior represent an upper bound for the stiffness modification factors found experimentally. However, the use of such factors in the repair design process may underestimate the displacement demands of the damaged structure and result in non-conservative designs.

4.7 Assessment of energy dissipation

Another metric that can be used to assess the effectiveness of the repair technique is through the computation of the equivalent viscous damping (ξ_{eq}). The total equivalent viscous damping, which is usually used in displacement-based seismic design or in assessment of structures (Priestley *et al*. 2007), was obtained in this study as the sum of a 5% elastic damping and the hysteretic

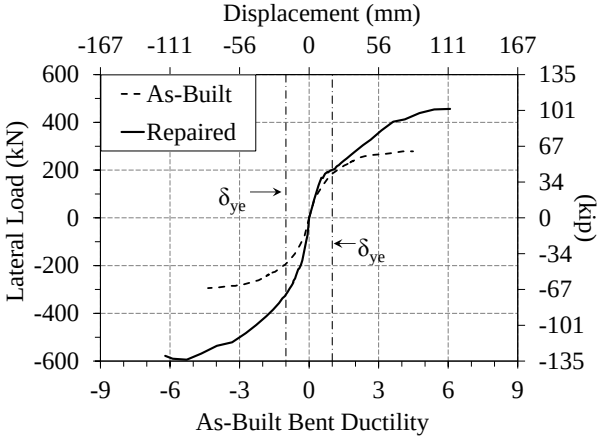

Fig. 16 Backbone curves comparison

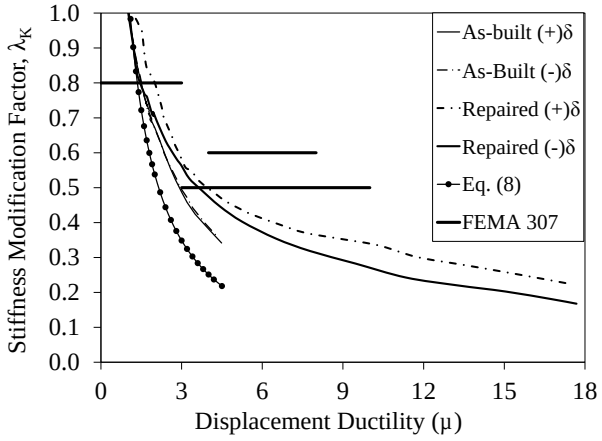

Fig. 17 Bent Stiffness

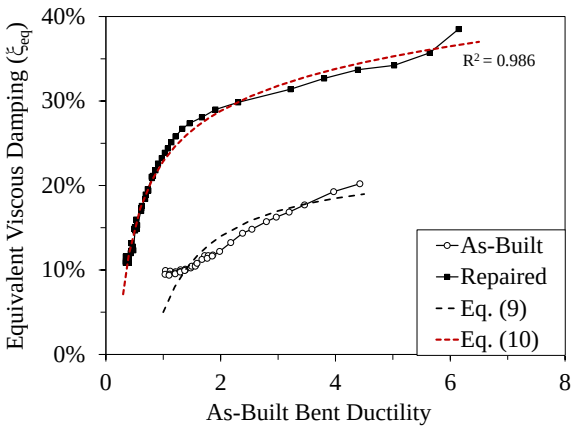

Fig. 18 Equivalent viscous damping

damping. The equivalent hysteretic damping was obtained from the experimental data as the ratio of the energy dissipated in a full cycle (A_d) to 4π times the strain energy ($\xi_{hys} = A_d/4\pi \cdot A_{strain}$). Fig. 18 summarizes the computed equivalent viscous damping for the tested specimens. The results show that the equivalent viscous damping for the repaired bent is on average 200% larger than for the original structure. Moreover, the repaired bent at ductility 1 had an equivalent viscous damping (24%), which is larger than the maximum damping attain for the As-built bent (20%). This result is consistent with the stable hysteretic behavior and full loops exhibited by the repaired bent and the subassemblage test of the BRB, and demonstrates that repairing damaged RC bents with ductile fuse bracing can result in high levels of energy dissipation.

Fig. 18 also shows a comparison of the experimental data for the as-built bent with the equivalent viscous damping for RC frames suggested by Priestley *et al*. (2007), which is given by Eq. (9). The figure shows that Eq. (9) tends to slightly overestimate the equivalent viscous damping of RC bridge bents in the ductility range of 2 to 3.5. Despite this slight overestimation, the equation provides a representative estimate of the equivalent viscous damping for bare RC structures.

$$\xi = 0.05 + 0.565 \cdot \left(\frac{\mu - 1}{\mu \cdot \pi}\right) \quad (9)$$

In addition, a regression analysis based on the experimental results of the repaired bent was performed in order to obtain Eq. (10), which can be used in the displacement-based seismic design of repaired structures with ductile steel braces.

$$\xi_{eq} = 0.927 \cdot \frac{(\mu - 0.2)^{1.14}}{\mu} \quad (10)$$

5. Conclusions

This study investigated the feasibility of repairing earthquake-damaged RC bridge bents with ductile fuse steel bracing, which was implemented using a buckling restrained brace. Implementation and design of the repair technique was outlined using a five step design methodology to achieve a desirable overall bent response. Large-scale cyclic experiments were used to validate the repair technique on a two column RC bent that was representative of commonly found deficient detailing in the Pacific Northwest of the United States. The bent was first tested in its as-built condition to impose damage and was then repaired using a BRB in a diagonal configuration. Cap beam strengthening was also needed based on the observed damage and was implemented with external post-tensioning. The following conclusions were obtained based on the observations and analysis of the experimental data:

- The As-built Bent test exhibited not only plastic hinge formation in the columns, but also formation of significant vertical cracks in the cap beam, which is indicative of plastic hinging. Plastic hinging in the cap beam is not desirable and generally prohibited by current seismic design specifications and required bent cap strengthening as part of the implemented repair.
- The experimental results demonstrated that repairing damaged RC bridge bents can be an effective technique to preserve bridge operation by limiting the spread of damage in the reinforced concrete components while restoring the stiffness and strength of the damaged structure, decrease the rate of stiffness deterioration, and improve the energy dissipation capacity of the system.
- The repaired bent exhibited only minor lateral strength deterioration despite of the columns sustaining significant damage prior to the repair. This result indicates that the columns continued to fully resist the imposed gravity loads. Moreover, no damage was observed in the cap beam at the end of testing, which demonstrated that post-tensioning of the cap beam was an effective method to strengthen and restrict the damage in that component.
- The contribution of the ductile steel bracing at the peak load of the repaired system was 73%, which demonstrated that majority of the system lateral load was resisted by the ductile bracing, even at large deformations.
- The brace alters the axial loads in the bent columns. While, in column 1 the effect was negligible as compared to the As-built condition, the axial load in column 2 was directly influenced. The contribution from the brace, and more specifically the high compression over-strength factor exhibited by the BRB, resulted in tension forces in column 2. This variation in axial forces underscores the importance of understanding the over-strength of the ductile steel brace, which needs to be properly accounted for in the bent repair design as these forces directly affect the subsequent assessment of other components.
- Subassemblage test of the steel brace corresponded closely with the brace response recorded during the repaired bent test and demonstrated the high level of energy dissipation that were attained.
- Stiffness modification factors used in the initial

design of the repair technique were based on FEMA307. However, the FEMA307 factors were shown to be the upper bounds for the experimentally obtained stiffness factors and their use may lead to non-conservative designs since lower displacement demands for the repaired bent would be predicted.

Acknowledgments

This paper is based upon research funded by the Oregon Department of Transportation (ODOT), whose support is gratefully acknowledged. The authors are also grateful to CoreBrace LLC for providing the buckling-restrained braces used in the study. Any opinions, findings, and conclusions or recommendations expressed in this paper are those of the authors and do not necessarily reflect the views of the sponsors.

References

Abdelnaby, A.E. (2017), "Fragility curves for RC frames subjected to Tohoku mainshock-aftershocks sequences", *J. Earthq. Eng.*, 1-19.

AISC 341-16 (2016), Seismic Provisions for Structural Steel Buildings, American Institute of Steel Construction, Chicago, IL, USA.

Bazaez, R. and Dusicka, P. (2016a), "Cyclic behavior of reinforced concrete bridge bent retrofitted with buckling restrained braces", *Eng. Struct.*, **119**, 34-48.

Bazaez, R. and Dusicka, P. (2016b), "Cyclic Loading for RC Bridge Columns Considering Subduction Megathrust Earthquakes", *J. Bridge Eng.*, **21**(5), 04016009.

Bazaez, R. and Dusicka, P. (2017), "Performance assessment of multi-column RC bridge bents seismically retrofitted with buckling-restrained braces", *Bull. Earthq. Eng.* DOI: https://doi.org/10.1007/s10518-017-0279-3

Chai, Y.H., Priestley, M.J.N. and Seible, F. (1991), "Retrofit of Bridge Columns for Enhanced Seismic Performance", *Seismic Assessment and Retrofit of Bridges*, Issue SSRP 91/03, pp. 177-196.

Chang, S., Li, Y. and Loh, C. (2004), "Experimental Study of Seismic Behaviors of As-Built and Carbon Fiber Reinforced Plastics Repaired Reinforced Concrete Bridge Columns", *J. Bridge Eng.*, **9**(4), 391-402.

Cheng, C., Yang, J., Yeh, Y. and Chen, S. (2003), "Seismic performance of repaired hollow-bridge piers", *Constr. Build. Mater.*, **17**(5), 339-351.

Di Ludovico, M., Polese, M., d'Aragona, M.G., Prota, A. and Manfredi, G. (2013), "A proposal for plastic hinges modification factors for damaged RC columns", *Eng. Struct.*, **51**, 99-112.

Dong, Y. and Frangopol, D.M. (2015), "Risk and resilience assessment of bridges under mainshock and aftershocks incorporating uncertainties", *Eng. Struct.*, **83**, 198-208.

El-Bahey, S. and Bruneau, M. (2011), "Buckling restrained braces as structural fuses for the seismic retrofit of reinforced concrete bridge bents", *Eng. Struct.*, **33**(3), 1052-1061.

Fakharifar, M., Chen, G., Wu, C., Shamsabadi, A., ElGawady, M. and Dalvand, A. (2016), "Rapid Repair of Earthquake-Damaged RC Columns with Prestressed Steel Jackets", *J. Bridge Eng.*, **21**(4), 04015075.

FEMA306 (1998), Evaluation of Earthquake Damaged Concrete and Masonry Wall Buildings, s.l.: Applied Technology Council (ATC-43 Project), The Partnership for Response and Recovery.

FEMA307 (1998), Evaluation of Earthquake Damaged Concrete and Masonry Wall Buildings - Technical Resources, s.l.: Federal Emergency Management Agency.

He, R., Grelle, S., Sneed, L. and Belarbi, A. (2013), "Rapid repair of a severely damaged RC column having fractured bars using externally bonded CFRP", *Compos. Struct.*, **101**, 225-242.

Jeon, J.S., DesRoches, R. and Lee, D.H. (2016), "Post-repair effect of column jackets on aftershock fragilities of damaged RC bridges subjected to successive earthquakes", *Earthq. Eng. Struct. Dyn.*, **45**(7), 1149-1168.

Kam, W.Y., Pampanin, S. and Elwood, K. (2011), "Seismic performance of reinforced concrete buildings in the 22 February Christchurch (Lyttleton) earthquake", *Bull. New Zealand Soc. Earthq. Eng.*, **44**(4), 239-278.

Kawashima, K. and Buckle, I. (2013), "Structural performance of bridges in the Tohoku-Oki earthquake", *Earthq. Spectra*, **29**(S1), S315-S338.

Lehman, D., Gookin, S., Nacamuli, A. and Moehle, J. (2001), "Repair of Earthquake-Damaged Bridge Columns", *ACI Struct. J.*, **98**(2), 233-242.

NCHRP (2013), Performance-Based Seismic Bridge Design, Synthesis 440, Transportation Research Board, National Academy of Sciences, Washington, D.C., USA.

Priestley, M., Seible, F. and Calvi, G. (1996), *Seismic Design and Retrofit of Bridges*, Wiley, New York, NY, USA.

Priestley, M.J.N., Calvi, G.M. and Kowalsky, M.J. (2007), Displacement-based seismic design of structures, s.l.: IUSS Press, Italy.

Saadatmanesh, H., Ehsani, M. and Jin, L. (1997), "Repair of Earthquake-Damaged RC Columns with FRP Wraps", *ACI Struct. J.*, **94**(2), 206-214.

Shin, M. and Andrawes, B. (2011), "Emergency repair of severely damaged reinforced concrete columns using active confinement with shape memory alloys", *Smart Mater. Struct.*, **20**(6), 065018.

Vosooghi, A. and Saiid Saiidi, M. (2013), "Design Guidelines for Rapid Repair of Earthquake-Damaged Circular RC Bridge Columns Using CFRP", *J. Bridge Eng.*, **18**(9), 827-836.

Wang, Y., Ibarra, L. and Pantelides, C. (2016), "Seismic Retrofit of a Three-Span RC Bridge with Buckling-Restrained Braces", *J. Bridge Eng.*, **21**(11), 04016073.

Wei, X. and Bruneau, M. (2016), "Case Study on Applications of Structural Fuses in Bridge Bents", *J. Bridge Eng.*, **21**(7), 05016004.

BU